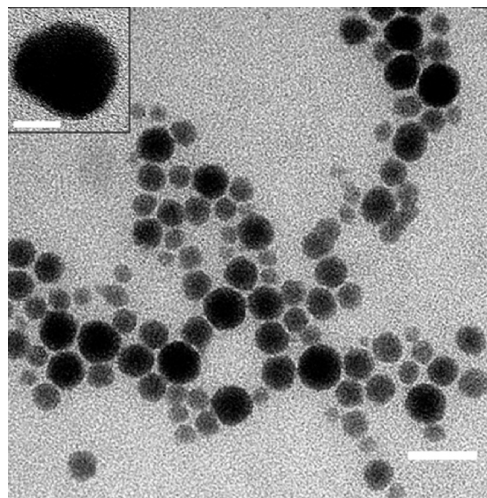


# Characterization of Antiplatelet Properties of Silver Nanoparticles

Siddhartha Shrivastava,<sup>†,¶</sup> Tanmay Bera,<sup>\*,¶</sup> Sunil K. Singh,<sup>†</sup> Gajendra Singh,<sup>§</sup> P. Ramachandrarao,<sup>⊥</sup> and Debabrata Dash<sup>†,\*</sup>

<sup>†</sup>Department of Biochemistry, Institute of Medical Sciences, Banaras Hindu University, Varanasi-221005, India, <sup>‡</sup>Department of Metallurgy, Institute of Technology, Banaras Hindu University, Varanasi-221005, India, <sup>§</sup>Department of Anatomy, Institute of Medical Sciences, Banaras Hindu University, Varanasi-221005, India, and <sup>⊥</sup>International Advanced Research Centre for Powder Metallurgy and New Materials, Balapur, Hyderabad-500 005, India. <sup>¶</sup>These authors have contributed equally to this work.

**P**latelet activation is a precisely regulated event critical for physiological blood flow. Although it serves an important role in control of hemorrhage, any hyperactivity leads to disease. Indeed, patients with cardiovascular and cerebrovascular disorders are reported to have more reactive platelets than their normal counterparts. Thrombotic disorders have emerged as serious threats to society as they are accompanied by significant morbidity and mortality. Anticoagulant and thrombolytic therapy like intravenous heparin treatment,<sup>1</sup> tissue plasminogen activator, urokinase, or streptokinase<sup>2</sup> play crucial roles in the management of patients; however, these are not safe<sup>3–6</sup> and may lead to serious bleeding complications associated with reocclusion and reinfarction. As platelets play a central role in thrombotic disorders, the focus has now shifted to regulating and maintaining these cells in an inactive state.<sup>7</sup>



**Figure 1.** Morphology of silver nanoparticles. Electron micrograph of silver nanoparticles showing spherical, monodispersed particles (scale bar, 30 nm). Inset shows one single particle of silver (scale bar, 5 nm).

**ABSTRACT** Thrombotic disorders have emerged as serious threat to society. As anticoagulant and thrombolytic therapies are usually associated with serious bleeding complications, the focus has now shifted to regulating and maintaining platelets in an inactive state. In the present study we show that nanosilver has an innate antiplatelet property and effectively prevents integrin-mediated platelet responses, both *in vivo* and *in vitro*, in a concentration-dependent manner. Ultrastructural studies show that nanosilver accumulates within platelet granules and reduces interplatelet proximity. Our findings further suggest that these nanoparticles do not confer any lytic effect on platelets and thus hold potential to be promoted as antiplatelet/antithrombotic agents after careful evaluation of toxic effects.

**KEYWORDS:** silver nanoparticles · antiplatelet · platelet aggregation · phosphotyrosine

Antiplatelet drugs like inhibitors of P2Y<sub>12</sub> receptor, integrin  $\alpha_{IIb}\beta_3$ , cyclooxygenase, and phosphodiesterase are also widely used in therapy but with serious limitations. Phosphatidylinositol 3-kinase inhibitors have been proposed as potential anti-thrombotic therapy<sup>8</sup> in view of the role of this enzyme in platelet activation and plug stability;<sup>9–12</sup> however, these too have major limitations for use as drugs.

Nanoparticles, on the contrary, can be synthesized and assembled in various shapes, sizes, and architectures, which leads to achieving the required properties. They are also amiable to biological functionalization. Thus, they have potential biological and medical applications.<sup>13–17</sup> The size of these particles can be suitably manipulated to enable them to pass through biological membranes and affect cell physiology,<sup>18</sup> which has been a challenge for the traditional medicines. We have recently reported synthesis of highly stable, uniformly sized silver nanoparticles endowed with enhanced antibacterial properties.<sup>19</sup> These particles may interact with bacterial proteins,

\*Address correspondence to ddass@satyam.net.in.

Received for review January 30, 2009 and accepted April 27, 2009.

Published online May 4, 2009.  
10.1021/nn900277t CCC: \$40.75

© 2009 American Chemical Society

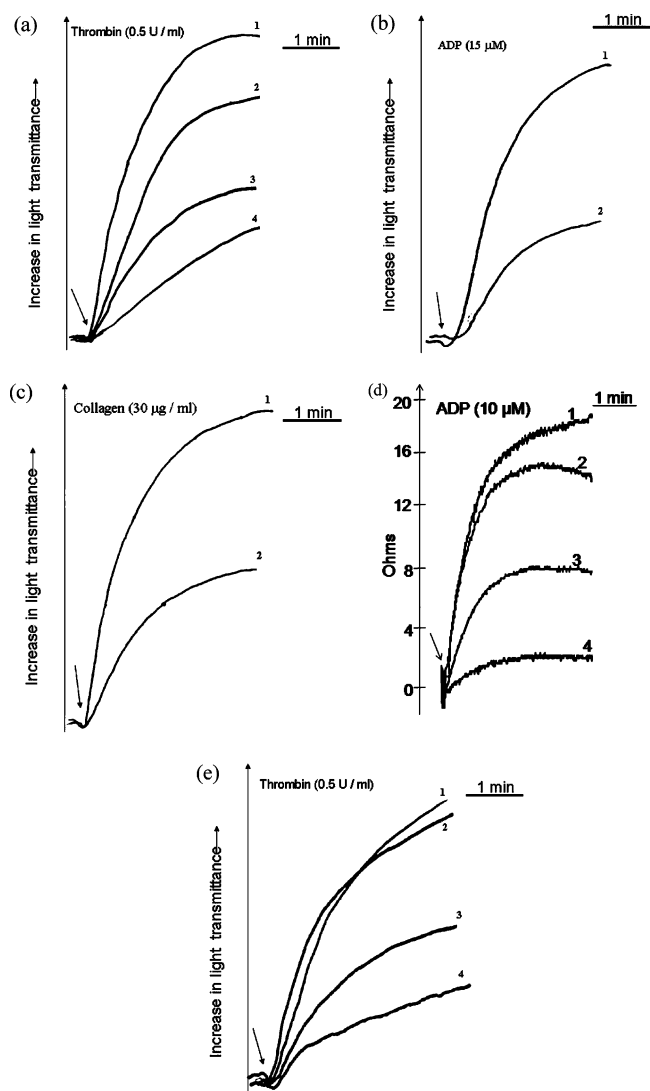


**Figure 2.** Effect of silver nanoparticles on platelet aggregation. (a) Tracings 1–4 denote aggregation in the presence of buffer or 0.5, 5, and 50  $\mu\text{M}$  of silver nanoparticles, respectively; (b, c) tracings 1 and 2 represent platelets pretreated with either buffer (control) or silver nanoparticles (50  $\mu\text{M}$ ), respectively; (d) tracings 1–4 denote platelet aggregation in whole blood (studied by electronic impedance) collected from mice, which were administered intravenously with vehicle or 4, 6, and 8 mg/kg body weight of silver nanoparticles, respectively. (e) Platelets were pretreated with either vehicle (tracings 1 and 2) or silver nanoparticles (50  $\mu\text{M}$ ) (tracings 3 and 4), followed by aggregation with thrombin. Tracings 1 and 4, aggregation of platelets without resuspension; tracings 3 and 4, aggregation of platelets following sedimentation and resuspension in fresh media. Results are representative of five individual experiments.

affecting cellular signaling mechanism.<sup>19</sup> Silver nanoparticles are capable of penetrating small capillaries following systemic administration<sup>18,20</sup> and are eliminated from the system by liver and kidneys. This opens up the possibility of delivering these nanomedicines to specific tissues with proper control. But toxicity of silver, as with any other nano preparation, remains a concern. Literature is inconclusive with regard to silver nanoparticles' impact on human health. There have been reports to suggest that nanoscale silver particles do not show significant signs of cytotoxicity<sup>21,22</sup> and exhibit

low toxicity in the human body.<sup>23,24</sup> Chronic ingestion or inhalation of silver preparations (especially colloidal silver) can lead to deposition of silver in the skin (argyria) or eye (argyrosis).<sup>23,25</sup> Although cosmetically undesirable, these are not life-threatening conditions. On the contrary, overexposure to nanosilver may lead to its accumulation and toxic changes in organs like liver, kidney, lungs, gingival mucous membrane, and spleen.<sup>22,26,27</sup> Silver in nano form has been reported to impair mitochondrial function in three murine cell lines.<sup>28–30</sup> There exists a report to suggest that nanotubes of carbon aggravate platelet aggregation,<sup>31</sup> but to the best of our knowledge there has been no study to investigate the effect of silver nanoparticles on platelet reactivity. In this report we show that nanoscale silver particles effectively prevent platelet aggregation, adhesion to immobilized matrix, and retraction of fibrin clot in a concentration-dependent manner. Administered intravenously, it protects mouse platelets from being aggregated in response to agonists. Our findings further suggest that silver nanoparticles do not confer any cytolytic effect on platelets and thus hold immense potential to be promoted as an antiplatelet agent.

## RESULTS AND DISCUSSION

**Characterization of Silver Nanoparticles.** Silver nanoparticles were synthesized through an aqueous chemical precipitation method, as described in our earlier report.<sup>19</sup> Nanoparticles were spherical in shape, 10–15 nm in diameter and monodispersed (Figure 1). Detailed procedure for synthesis and characterization are provided in the Supporting Information.

**Effect of Silver Nanoparticles on Platelet Functions.** Silver nanoparticles inhibited thrombin-induced platelet aggregation in a concentration-dependent manner (Figure 2a). The extent of inhibition was the same irrespective of whether platelets were aspirinized or not. More than 80% ( $n = 10$ ) inhibition in amplitude was recorded at a nanoparticle concentration of 50  $\mu\text{M}$ , which also significantly reduced the slope of aggregation per minute. Under the same condition platelet aggregation induced by other physiological agonists like ADP (adenosine diphosphate) and collagen was also significantly inhibited (Figure 2b,c). As these agonists act through different signaling routes, the site of action of silver nanoparticles appeared to be a step common to and downstream of these pathways.

Further we asked whether incubation with nanosilver would suppress abnormally active platelets from prothrombotic situations. Nanoparticles (50  $\mu\text{M}$ ) significantly inhibited aggregation of platelets obtained from patients with noninsulin-dependent diabetes mellitus by nearly 50% ( $n = 4$ ) (see Supporting Information). Adhesion of platelets under flow onto the immobilized collagen, mimicking the *in vivo* situation for thrombus generation, was also reduced significantly (by  $66 \pm 4\%$ ,  $P = 0.00002$ ,  $n = 5$ ) in the presence of nanoparticles

(50  $\mu\text{M}$ ). Moreover, intravenous administration of nanoparticles (2–8 mg/kg body weight) in two different mice strains led to significant inhibition of platelet aggregation in mouse whole blood (studied by electronic impedance) in a dose-dependent manner (Figure 2d), suggestive of potential antiplatelet effects of nanoparticles *in vivo*. Tail bleeding assays ruled out any adverse effect on bleeding time upon administration of nanoparticles to rodents. Mice survived normally after the dose treatment. This is also consistent with recent report that a dose of nanosilver up to 300 mg/kg was non-toxic to rodents.<sup>32</sup>

Next we asked whether inhibition of platelet aggregation by nanoparticles was attributable to their mere physical presence in the medium affecting platelet–platelet interaction, or was the outcome of specific modulation of platelet signaling pathways. Cells were incubated with silver nanoparticles, and then washed by sedimenting and resuspending them in fresh medium without nanoparticles. Control cells, which were treated similarly but without exposure to nanoparticles, displayed normal aggregation (Figure 2e, tracing 2). Aggregation was significantly reduced in platelets originally exposed to nanoparticles (Figure 2e, tracing 3), suggestive of sustained interaction between nanoparticles and platelets, as otherwise aggregation curves would have been comparable. Nanoparticles also significantly inhibited secretion from dense and alpha granules in thrombin-stimulated platelets when the cells were stirred (aggregated) (see Supporting Information), indicating modulation of integrin signaling by nanosilver.

Next we examined whether nanoparticles could prevent adhesion of platelets onto immobilized fibrinogen. Pretreatment with nanosilver (50  $\mu\text{M}$ ) significantly reduced the number of cells adhered onto fibrinogen (Figure 3a; a and b), whereas adhesion to poly-L-lysine was unaffected (not shown). Nanosilver had no effect on platelet spreading on fibrinogen (Figure 3a; c and d).

Subsequently we studied the effect of nanoparticles on fibrin clot retraction, which results from the interaction between platelet integrin  $\alpha_{\text{IIb}}\beta_3$  and fibrin. Pretreatment of platelets with increasing concentration of silver nanoparticles led to progressive inhibition in the extent of retraction (up to 40% inhibition in presence of 50  $\mu\text{M}$  nanosilver) (Figure 3b). Specific platelet proteins are known to become dephosphorylated on tyrosine during the process of clot retraction.<sup>33</sup> We examined whether failure to retract fibrin clot was associated with decreased protein tyrosine dephosphorylation in nanoparticle-treated platelets (Figure 3c). As expected, platelet proteins of  $M_r$  210, 125, 105, 80, and 55 kDa were dephosphorylated in the retracted clot (Figure 3c, lane 4). Pretreatment with increasing concentration of nanoparticles progressively restored phosphorylation of these proteins on tyrosine (Figure 3c, lanes 5–8).

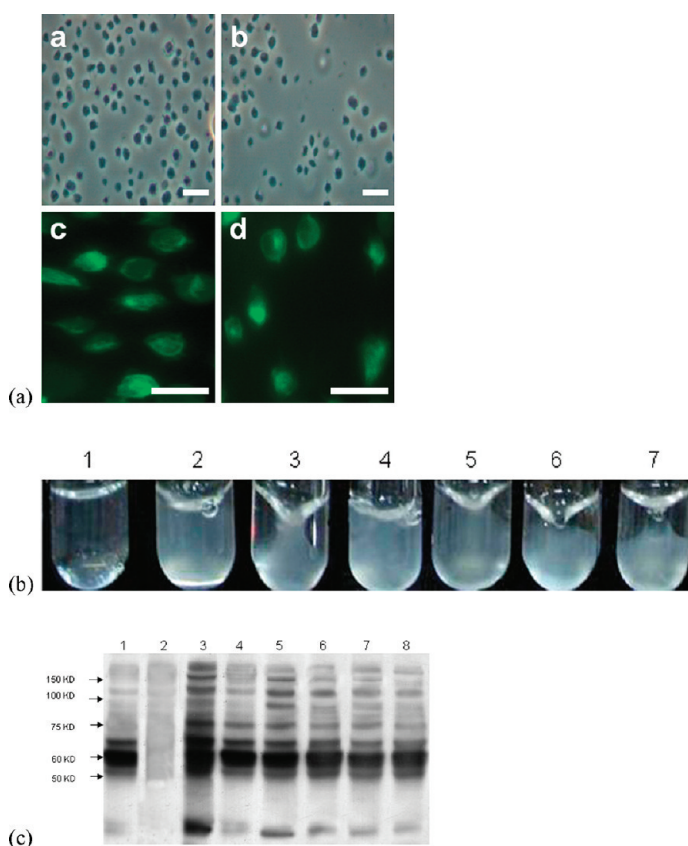


**Figure 3.** Effect of silver nanoparticles on integrin  $\alpha_{\text{IIb}}\beta_3$ -mediated platelet responses. (a) Adhesion and spreading of platelets on immobilized fibrinogen. Platelets were labeled with phalloidin-FITC and allowed to adhere on to immobilized fibrinogen. Adhesion (a and b) and spreading (c and d) of platelets were microscopically examined with phase contrast and fluorescence attachments, respectively. panels a and c show untreated platelets; panels b and d show silver nanoparticle (50  $\mu\text{M}$ )-pretreated platelets. Scale bars, 10  $\mu\text{m}$ . (b) Platelet mediated clot retraction. Tube 2, no retraction (calcium excluded); tube 3, full retraction; tubes 4–7, retraction in the presence of platelets pretreated with 50, 5, 0.5, and 0.05  $\mu\text{M}$  silver nanoparticles, respectively. Tube 1, no clot formation (thrombin excluded). Data are from a single experiment representative of five different experiments. (c) Phosphotyrosine protein profile in platelets associated with fibrin clot retraction. Lane 3, no retraction (calcium excluded); lane 4, full retraction; lanes 5–8, pretreatment of platelets with 50, 5, 0.5, and 0.05  $\mu\text{M}$  silver nanoparticles, respectively. Lane 1, resting platelets; lane 2, fibrin clot (platelets excluded). Blot is from a single experiment representative of five different experiments.

To understand the molecular basis underlying the antiplatelet effect, we studied tyrosine phosphoproteome in nanoparticle (50  $\mu\text{M}$ )-pretreated platelets. As expected, thrombin evoked phosphorylation of multiple proteins in stirred (aggregated) as well as unstirred platelets. Nanosilver precluded tyrosine phosphorylation of proteins in stirred samples (Figure 4a, lanes 2 and 3) under the condition in which aggregation was prevented (Figure 2a), and not in unstirred platelets (Figure 4a, lanes 4 and 5), implicating a critical role of integrin  $\alpha_{\text{IIb}}\beta_3$ . Next we incubated platelets with  $\text{MnCl}_2$ , which is known to bring about activation-specific conformational changes in  $\alpha_{\text{IIb}}\beta_3$ .<sup>34</sup> Consistent with earlier reports,<sup>35</sup>  $\text{Mn}^{2+}$  induced tyrosine phosphorylation of platelet proteins. Phosphorylation was significantly retarded in the presence of nanoparticles (Figure 4a, lanes



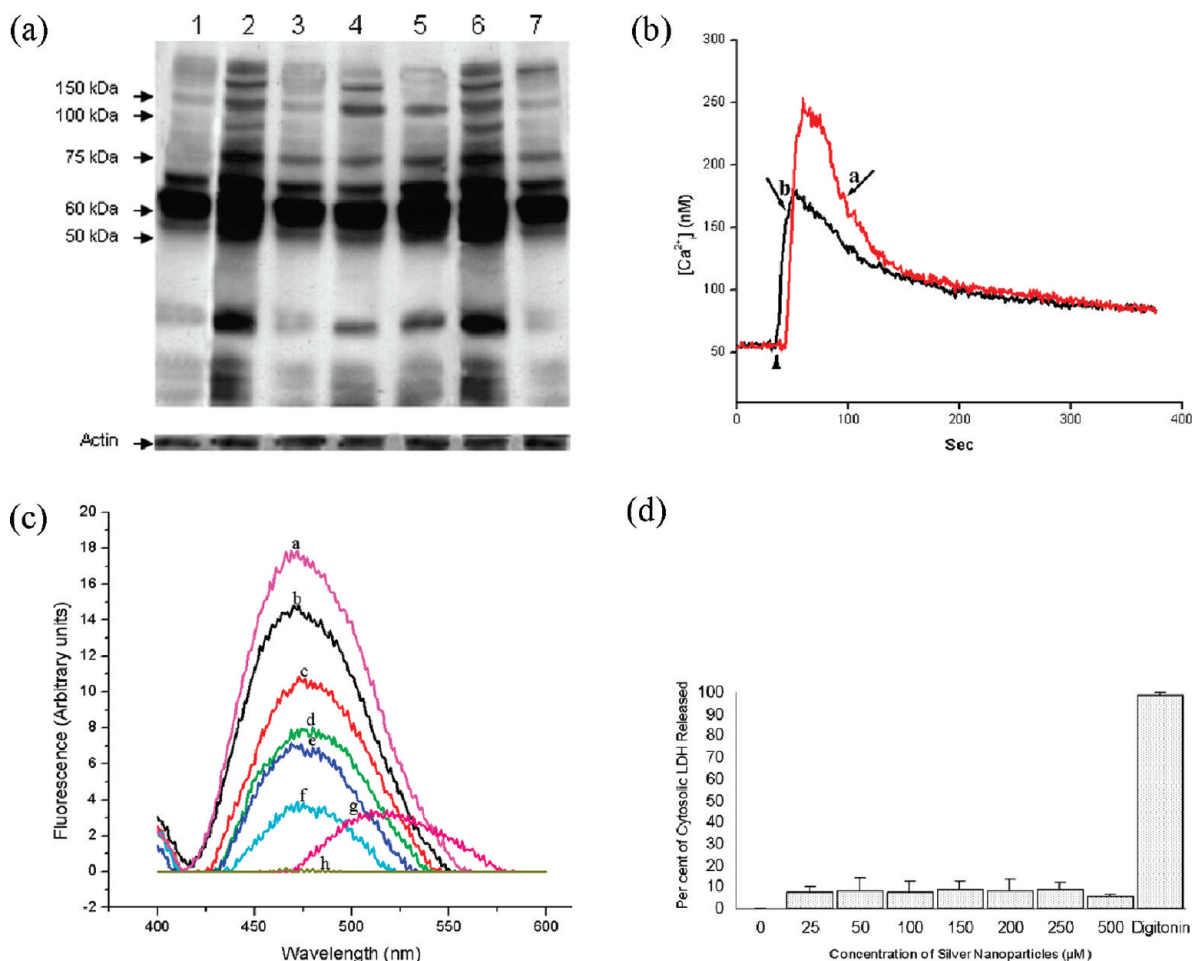


**Figure 4.** Effect of silver nanoparticles on signaling and membrane parameters of platelets. (a) Tyrosine phosphorylation of platelet proteins under different activation states of platelets. Upper panel, lane 1, resting platelets; lanes 2 and 3, thrombin-stimulated stirred (aggregated) platelets; lanes 4 and 5, thrombin-stimulated unstirred platelets; lanes 6 and 7, platelets activated with  $MnCl_2$ . Lanes 3, 5, and 7 represent platelets pretreated with nanosilver (50  $\mu$ M). Lower panel, Coomassie staining of blot showing presence of actin in equal amount in the lanes. (b) Intracellular calcium flux in thrombin-stimulated platelets. Fura-2 loaded platelets were treated either with buffer (tracing a) or with 50  $\mu$ M of silver nanoparticles (tracing b), followed by thrombin addition (arrowhead). (c) ANS binding to platelet membrane: (a) ANS bound to control platelets; (b, c, d, e, and f) ANS bound to platelets pretreated with 15, 25, 50, 150, and 250  $\mu$ M silver nanoparticles, respectively; (g) free ANS and (h) unlabeled platelets; excitation, 380 nm. (d) Study of membrane integrity. Leakage of LDH from platelet cytosol was studied in presence of different concentrations of silver nanoparticles as indicated and digonin (30  $\mu$ M). The result was representative of five independent experiments (mean  $\pm$  SD).

6 and 7), suggesting possible modulation of integrin conformation by nanosilver.

We next studied the effect of nanosilver on platelet cytosolic  $Ca^{2+}$ ,  $[Ca^{2+}]_i$ , a critical regulator of intracellular signaling. Thrombin evoked an initial 5-fold rise in  $[Ca^{2+}]_i$ , followed by a plateau. Pretreatment of platelets with nanoparticles (50  $\mu$ M) led to significant fall in the initial rise in  $[Ca^{2+}]_i$ , suggestive of reduced release of  $Ca^{2+}$  from the intracellular stores (Figure 4b).

As platelet stimulation is associated with extensive reorganization of actin-based cytoskeleton,<sup>36–38</sup> we investigated the effect of nanoparticles on actin polymerization. Nanosilver (50  $\mu$ M) significantly suppressed thrombin-induced rise in platelet F-actin, suggestive of interference with barbed-end polymerization (see Supporting Information). To examine the effect of silver nanoparticles on physical microenvironment of plate-

let membrane, we studied affinity of ANS (1-anilino-8-naphthalene sulfonate), an anionic fluorescent probe, toward membrane. Upon binding the emission peak of ANS was blue-shifted from 520 to 480 nm accompanied by intensity enhancement. Pretreatment of platelets with nanosilver elicited progressive decrease in fluorescence intensity in a dose-dependent manner, the emission maximum remaining unchanged (Figure 4c). Quenching of fluorescence could be attributed either to decreased quantum yield of bound ANS or to reduction in the number of ANS molecules bound. Since ANS binding reflects membrane surface charge, packing effect, and degree of lipid disorder,<sup>39</sup> nanosilver appeared to contribute significantly to platelet membrane disorder.

We subsequently explored possible cytotoxic effects of nanoparticles by examining leakage of cyto-

lic LDH (lactate dehydrogenase). Nanoparticles (25 to 500  $\mu\text{M}$ ) did not elicit any significant release of LDH from platelet cytosol, whereas exposure to digitonin (30  $\mu\text{M}$ ) brought about extrusion of more than 90% of LDH (Figure 4d). Thus, silver nanoparticles, even at higher concentration, did not affect platelet membrane integrity or cause cell lysis, though membrane order was disturbed.

Interaction between platelets and silver nanoparticles was further examined by transmission electron microscopy (Figure 5). Figure 5a shows intact activated platelets with characteristic well-developed hyaloplasmic processes (pseudopods), dense granules (DG) with eccentric opacity, and vacuoles (V) with limiting membrane. In nanosilver-treated samples most of the available vacuolar and granular spaces were seen occupied with nanoparticles, which were also distributed in interplatelet spaces (Figure 5b). Hyaloplasmic processes were scarcer in nanoparticle-pretreated cells. Aggregated platelets were seen intimately adhered to each other (Figure 5c), which led to stable plaque and thrombus formation. Nanoparticle (50  $\mu\text{M}$ )-pretreated platelets failed to aggregate and could only manage to form small, diffuse, and loosely packed clumps separated by wide distances (Figure 5d).

To relate nanoparticle size with antiplatelet effects, we studied platelet aggregation in the presence of nanosilver (50  $\mu\text{M}$ ) having different sizes (see Supporting Information). Consistent with recent reports,<sup>40,41</sup> silver nanoparticles (13–15, 30–35, and 40–45 nm size ranges, respectively) inhibited aggregation by similar extents. Next, we asked whether the observed antiplatelet properties were inherent to silver material or shared with other metal nanoparticles as well. Pretreatment with 50  $\mu\text{M}$  gold nanoparticles (13, 20, and 29 nm sizes) was found to have no effect on platelet aggregation (see Supporting Information), suggestive of unique antiplatelet property endowed in nanosilver, in addition to its well-documented antibacterial property.<sup>19</sup>

## CONCLUSION

In summary, we demonstrated here that silver nanoparticles effectively inhibited integrin-mediated platelet functional responses like aggregation, secretion, adhesion to immobilized fibrinogen or collagen and

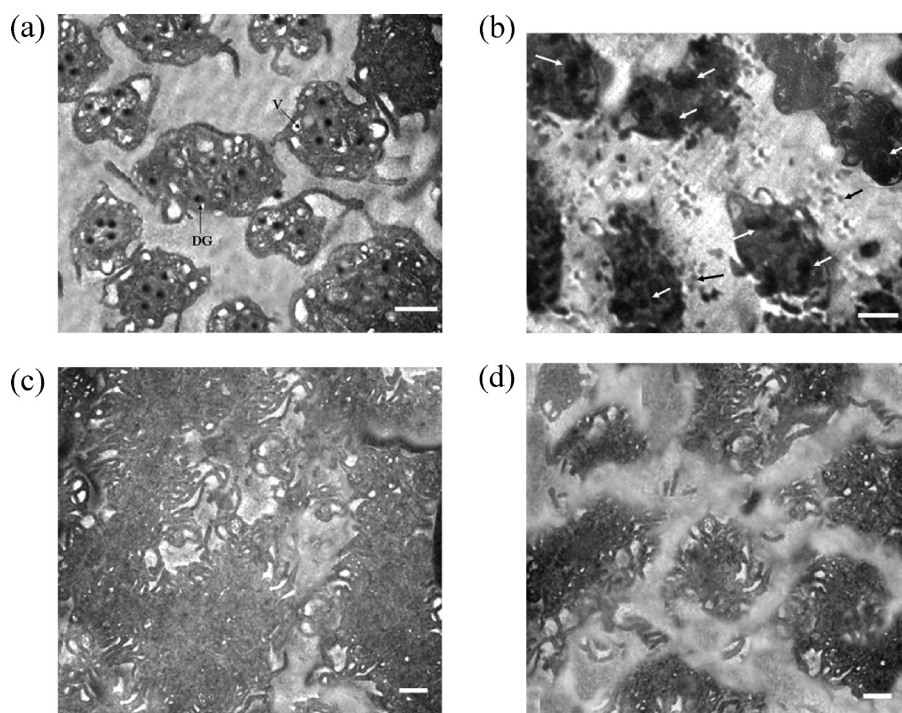


**Figure 5.** Electron micrographs through sections of activated and aggregated platelets with and without pretreatment of silver nanoparticles (50  $\mu\text{M}$ ). (a) Intact platelets showing hyaloplasmic processes (pseudopods), dense granules (DG) with eccentric opacity, and vacuoles (V) with limiting membrane. (b) Platelets pretreated with silver nanoparticles showed accumulation of nanoparticles in vacuolar spaces (white arrow) with the absence of hyaloplasmic processes. Nanoparticle clusters (black arrow) are also seen in the surrounding microenvironment. (c) Electron micrograph demonstrating intimate adherence between the platelets during thrombus formation. Only occasional narrow spaces are visible between some cells. (d) Silver nanoparticle-pretreated platelets failed to aggregate and could only manage to form small, diffuse, and loosely packed clumps separated by wide distances. Scale bars, 1  $\mu\text{m}$  (a and b) and 10  $\mu\text{m}$  (c and d).

retraction of fibrin clot in a dose-dependent manner, irrespective of the nature of agonists used. *In vivo* studies using mouse models also supported antiplatelet properties of nanosilver, which were innate to silver and not exhibited by gold nanoparticles of comparable sizes. Chances of nanosilver transforming into  $\text{Ag}^+$  inside the platelets were rare in view of high ionization potential of silver (735 kJ/mol), which is difficult to be achieved in the intracellular environment, thus indicating that the observed effects were the result of direct interaction of nanosilver with platelet machinery. Studies using  $\text{MnCl}_2$  suggested that the inhibition could be due to conformational modulation of platelet surface integrins  $\alpha_{\text{IIb}}\beta_3$ , thus preventing the latter's interaction with fibrinogen. This also explains changes in outside-in signaling parameters like altered platelet phosphoproteome in nanoparticle-treated platelets. In agreement with this, signaling pathways unrelated to integrin ligation and clustering, those observed using unstirred (nonaggregated) thrombin-stimulated platelets, were mostly unaffected by the presence of nanoparticles.

ANS binding as well as electron microscopic data suggested that nanosilver had a perturbing effect on platelet membrane microenvironment. It occupied platelet granules and vacuolar spaces and prevented hyaloplasmic extensions with diminished interplatelet

proximity. Platelets did not release intracellular LDH even after exposure to a considerably high concentration of nanoparticles reflecting lack of cell lysis and sustenance of membrane integrity. Silver nanoparticles also suppressed the aggregation of platelets obtained from patients with type 2 diabetes mellitus. Thus, significant inhibition of platelet functions with a relatively low dose of nanosilver, combined with the lack of cell

lysis, raise the hope for its use as an antiplatelet therapeutic agent. It may be used effectively with coronary stents, where the antibacterial property of nanosilver would complement its antiplatelet potency. However, like all nascent medicines and medical devices critical appraisal of benefits and side effects of nanosilver with intense cytotoxicity studies<sup>26,30,42</sup> will be required to guarantee its safety as a therapeutic agent.

## METHODS

**Platelet Preparation.** Platelets were isolated by differential centrifugation from fresh human blood, as already described.<sup>43</sup> Briefly, blood from healthy volunteers was collected in citrate–phosphate–dextrose adenine and centrifuged at 180g for 20 min. PRP (platelet-rich plasma) was incubated with 1 mM acetylsalicylic acid for 15 min at 37 °C. After the addition of EDTA (ethylenediaminetetraacetic acid) (5 mM), platelets were sedimented by centrifugation at 800g for 15 min. Cells were washed in buffer A (20 mM Hepes, 138 mM NaCl, 2.9 mM KCl, 1 mM MgCl<sub>2</sub>, 0.36 mM NaH<sub>2</sub>PO<sub>4</sub>, 1 mM EGTA (ethylene glycol tetraacetic acid), supplemented with 5 mM glucose, and 0.6 ADPase units of apyrase/mL, pH 6.2). Platelets were finally resuspended in buffer B (pH 7.4), which was the same as buffer A but without EGTA and apyrase. The final cell count was adjusted to (0.5–0.8) × 10<sup>9</sup>/mL. All steps were carried out under sterile conditions, and precautions were taken to maintain the cells in an inactivated state.

**Synthesis of Nanoparticles.** Silver nanoparticles were synthesized essentially as described in our earlier report.<sup>19</sup> Details of synthesis of silver and gold nanoparticles are provided in Supporting Information.

**Platelet Aggregation and Activation Studies.** Platelets were stirred (1200 rpm) at 37 °C in a Chrono-log platelet ionized calcium aggregometer (model 600) for 2 min prior to the addition of agonists. Wherever indicated, cells were stimulated without stirring to prevent aggregation. For experiments using ADP as the agonist, platelets were prepared without exposure to acetylsalicylic acid and were incubated with fibrinogen (0.1 mg/mL) prior to the addition of agonist. Aggregation was measured as percent change in light transmission, where 100% refers to transmittance through blank sample. In other experiments platelets were activated by incubating the cells with 250 μg/mL fibrinogen and freshly prepared MnCl<sub>2</sub> (1 mM) for 15 min at 37 °C. Finally, cells were boiled in Laemmli lysis buffer and stored at –20 °C until further analysis.

To examine the effect of nanoparticles on platelet aggregation, cells were incubated for 2 min at 37 °C in the presence of 50 μM silver or gold nanoparticles of different sizes prior to the addition of agonist. In other experiments platelet-nanoparticle interaction was studied by incubating the cells in the presence or absence of nanoparticles (50 μM), sedimenting, and resuspending the cells in Buffer B (without nanoparticles), followed by stimulation with thrombin.

**Platelet Adhesion and Spreading Studies.** To study platelet adhesion to immobilized matrix, control cells as well as cells pretreated with nanoparticles were fixed with 4% paraformaldehyde. Cells were charged onto slides coated either with poly-L-lysine (0.01% w/v) or fibrinogen (100 μg/mL), incubated for 30 min at room temperature (RT) followed by washing. The adhered cells were observed under fluorescence microscope with phase contrast attachment (Leica, model DM LB2) at 100× in oil. Time-lapse events were captured by Leica DFC 320 CCD camera using IM50 software (Leica).

For spreading experiments, platelets (control, as well as nanoparticle-treated) were allowed to spread on fibrinogen-coated slides for 60 min at RT, followed by fixation with paraformaldehyde (4%). Cells were then permeabilized and incubated in the dark for 60 min at RT in the presence of phalloidin-FITC (fluorescein isothiocyanate) (1 μM) in 0.2% Triton X-100, fol-

lowed by washing. The spreading of platelets was recorded under the fluorescence microscope.

**Platelet Adhesion under Flow.** Platelets (3.5 × 10<sup>8</sup>/mL), either with or without nanoparticle pretreatment, were allowed to pass through 15 cm long polypropylene tubes (2 mm diameter), precoated with 50 μg/mL collagen, for 1 h at RT. Cells were counted before and after passage against immobilized collagen, and adhesion percentage was calculated.

**Platelet Secretion Studies.** Control as well as nanoparticle-treated platelets were stimulated with thrombin (0.5 U/mL) for 3 min. Aggregated (stirred) and activated (unstirred) platelet samples were centrifuged at 800g for 1 min in presence of 1 mM EDTA to prevent further platelet activation. Supernatants were added to reaction mixture containing luciferin–luciferase in microplates (Lumitrac 200, Greiner). Luminescence from the reaction of released adenine nucleotides was read in a luminescence microplate reader (BioTek, model FLx800TBI).

**In Vivo Studies with Silver Nanoparticles.** Fifty male mice (25 each from AKR and PARKES strains), 7–8 weeks old with average weight of 27 ± 3 g, were divided into groups consisting of five animals each. Intravenous injections of silver nanoparticles (2, 4, 6, and 8 mg/kg body weight, respectively) were slowly administered into tail veins of different groups of animals. After 10 min blood was collected by carotid puncture into heparinized tubes. Platelets were stimulated with 10 μM ADP and aggregation was measured in whole blood by electronic impedance in a Chrono-log Whole Blood/Optical Lumi-Aggregometer (model 700-2). For tail bleeding assay mice were anesthetized after intravenous injections of silver nanoparticles or vehicles and a 3 mm segment of the tail tip was cut off with a scalpel. Tail bleeding was monitored by gently absorbing the bead of blood with a filter paper without contacting the wound site. When no blood was observed on the paper after 15 s intervals, bleeding was determined to have ceased. The experiment was stopped after 15 min. Animal studies were carried out strictly as per the recommendations of the “Laboratory Animals Division”, Central Drug Research Institute, India, and the “Laboratory Animal Welfare Committee” of the University.

**Clot Retraction Studies.** Fibrinogen (2 mg/mL) was incubated with washed platelets (either control, or pretreated with varying concentrations of silver nanoparticles) in the presence of calcium (2 mM). Clot formation was induced by the addition of thrombin (1 U/mL). The clot was allowed to retract for 60 min at 37 °C. In control experiments retraction was prevented by the omission of calcium in the reaction mixture. Clots were lysed by boiling in the presence of Laemmli buffer for 20 min<sup>31</sup> and stored at –20 °C until further analysis.

Clot retraction was assessed by analyzing the digital photos with ImageJ 1.36b software (NIH, USA, <http://rsb.info.nih.gov/ij/>). The extent of retraction was expressed as a percentage of retraction defined as  $[1 - (\text{area } t / \text{area } t_0) \times 100]$ , where area  $t_0$  was the area occupied by the fibrin clot in the absence of platelets (‘negative control’) and area  $t$  was the area occupied by the retracted fibrin clot.<sup>44</sup>

**Flow Cytometry.** Platelets (2 × 10<sup>8</sup> cells in 200 μL) were incubated at 37 °C for 5 min without stirring in the presence of an agonist, either in the presence or absence of silver nanoparticles (50 μM), followed by the addition of an equal amount of 4% paraformaldehyde for 30 min. Cells were then washed and resuspended in buffer B and incubated with 2 μL PE-labeled antibody against P-selectin for 60 min in ice in the dark. Samples



were again washed with PBS and analyzed in a Becton Dickinson FACSCalibur flow cytometer.

**Immunoblotting Studies.** Platelet proteins were separated on 10% SDS-PAGE (sodium dodecyl sulfate polyacrylamide gel electrophoresis) gels and electrophoretically transferred to PVDF (polyvinylidene fluoride) membrane by using TE 77 PWR semi-dry system (GE Healthcare). Membranes were blocked with 5% bovine serum albumin in 10 mM Tris-HCl, 150 mM NaCl, pH 8.0 (TBS) containing 0.05% Tween-20 for 2 h at room temperature. Blots were incubated for 2 h with monoclonal antibody against phosphotyrosine (clone 4G10) at 1  $\mu$ g/mL, followed by horseradish peroxidase-labeled antimouse IgG for 1 h. Antibody binding was detected using enhanced chemiluminescence and quantified in an Agfa Duoscan T1200 flatbed scanner using Gene Tools software (Syngene).

**Measurement of F-Actin Content in Platelets.** The F-actin contents of resting and activated cells, with and without prior treatment with nanosilver (50  $\mu$ M) or cytochalasin D (10  $\mu$ M), were determined from the extent of phalloidin-FITC staining. Cells were fixed with equal volume of 4% paraformaldehyde at 37  $^{\circ}$ C for 30 min, followed by permeabilization at RT for 60 min in presence of 0.1% Triton-X-100 containing 10  $\mu$ M phalloidin-FITC in dark. Fluorescence was quantified in a Hitachi fluorescence spectrophotometer (model F-2500) using FL solutions software. Excitation and emission wavelengths were set at 496 and 516 nm, respectively.

**Measurement of Intracellular Free Calcium.** PRP was incubated with 2  $\mu$ M Fura-2 AM for 45 min at 37  $^{\circ}$ C in the dark. The Fura 2-loaded platelets were washed and resuspended in buffer B at  $10^8$  cells/mL. Fluorescence was recorded in 400  $\mu$ L aliquots of platelet suspensions, both control and those pretreated with 50  $\mu$ M silver nanoparticles, at 37  $^{\circ}$ C under nonstirring conditions. Excitation wavelengths were 340 and 380 nm and emission wavelength was set at 510 nm. Changes in intracellular free calcium concentration,  $[Ca^{2+}]_i$ , upon thrombin stimulation (1 U/mL) were monitored from the fluorescence ratio (340/380) using Intracellular Cation Measurement Program in FL Solutions software. Intracellular free calcium was calibrated according to the derivation of Grynkiewicz et al.<sup>45</sup>

**ANS Binding Study.** Effect of nanosilver on platelet membrane microenvironment was studied by labeling the cells with ANS. Labeling was done by adding the probe (5  $\mu$ M final concentration) to the platelet suspension ( $0.5 \times 10^8$ /mL) at RT.<sup>39</sup> Fluorescence emission spectra were recorded at 30  $^{\circ}$ C at an excitation of 380 nm.

**Measurement of LDH Leakage.** Control platelets, and platelets treated either with nanosilver (50  $\mu$ M) or with digitonin (30  $\mu$ M), were pelleted by centrifugation at 800g for 10 min. Supernatants were preserved and pellets were resuspended in identical volume of buffer B, followed by sonication. The reaction was initiated by the addition of platelet supernatant or sonication of (40–500  $\mu$ L) reaction mixtures containing 0.168 mM NADH and 32.52 mM sodium pyruvate at 30  $^{\circ}$ C. LDH activity was assayed from the time course of decrease in NADH absorbance at 340 nm.

**Transmission Electron Microscopy.** Different platelet samples, either with or without nanoparticle pretreatment, were fixed in Karnovsky fixative, postfixed in osmium, and stained with uranyl acetate. Blocks were prepared as previously described.<sup>46,47</sup> Thin sections (0.02  $\mu$ m thick) were made with an ultramicrotome (Leica, EM UC6). Samples were mounted on Formvar-coated grids, stained with lead citrate, and examined under a Technai-12 electron microscope equipped with SIS Mega View III CCD camera at 120 KV. Measurements were done using AnalySIS software (SIS, Germany).

**Statistical Methods.** Standard statistical methods were used. Parametric methods (*t* test) were used for evaluation and significance tests were considered significant at *P* less than 0.05 (2-tailed tests). Data are presented as means  $\pm$  SD of at least five individual experiments from different blood donors. Immunoblots shown are representatives of at least three different experiments.

**Acknowledgment.** This research was supported in part by grants received by D. Dash from the Department of Biotechnology (DBT), Government of India, and the DST Unit on Nano-

science and Technology (DST-UNANST), Banaras Hindu University. A donation from the Alexander von Humboldt-Stiftung, Germany, is gratefully acknowledged.

**Supporting Information Available:** Materials used, nanoparticle synthesis, and characterization details, description of the effect of silver nanoparticles on platelet secretion, actin polymerization, and on platelet aggregation from diabetic blood. This material is available free of charge via the Internet at <http://pubs.acs.org>.

## REFERENCES AND NOTES

- Watson, R. D.; Chin, B. S.; Lip, G. Y. Antithrombotic Therapy in Acute Coronary Syndromes. *Br. Med. J.* **2002**, *325*, 1348–1351.
- Baruah, D. B.; Dash, R. N.; Chaudhari, M. R.; Kadam, S. S. Plasminogen Activators: A Comparison. *Vasc. Pharmacol.* **2006**, *44*, 2–17.
- Patel, S. C.; Mody, A. Cerebral Hemorrhagic Complications of Thrombolytic Therapy. *Progress Cardiovasc. Dis.* **1999**, *42*, 217–233.
- Haines, S. T.; Busse, H. I. Thrombosis and the Pharmacology of Antithrombotic Agents. *Ann. Pharmacother.* **1995**, *29*, 892–904.
- Arcasoy, S. M.; Kreit, J. W. Thrombolytic Therapy of Pulmonary Embolism. *Chest* **1999**, *115*, 1695–1707.
- Khalid, A. Is Thrombolytic Therapy Effective for Pulmonary Embolism. *Am. Fam. Physician* **2002**, *65*, 1097–1102.
- Severin, S.; Gratacap, M. P.; Lenain, N.; Alvarez, L.; Hollande, E.; Penninger, J. M.; Gachet, C.; Plantavid, M.; Payrastre, B. Deficiency of Src Homology 2 Domain-Containing Inositol 5-Phosphatase 1 Affects Platelet Responses and Thrombus Growth. *The Journal of Clinical Investigation* **2007**, *117*, 944–952.
- Maxwell, M. J.; Yuan, Y.; Anderson, K. E.; Hibbs, M. L.; Salem, H. H.; Jackson, S. P. SHIP1 and Lyn Kinase Negatively Regulate Integrin  $\alpha_{IIb}\beta_3$  Signaling in Platelets. *J. Biol. Chem.* **2004**, *279*, 32196–32204.
- Watanabe, N.; Nakajima, H.; Suzuki, H.; Oda, A.; Matsubara, Y.; Moroi, M.; Terauchi, Y.; Kadowaki, T.; Koyasu, S.; Ikeda, Y.; Handa, M. Functional Phenotype of Phosphoinositide 3-Kinase p85 $\alpha$ -Null Platelets Characterized by an Impaired Response to GP VI Stimulation. *Blood* **2003**, *102*, 541–548.
- Yap, C. L.; Anderson, K. E.; Hughan, S. C.; Doppeide, S. M.; Salem, H. H.; Jackson, S. P. Essential Role for Phosphoinositide 3-Kinase in Shear-Dependent Signaling between Platelet Glycoprotein Ib/V/IX and Integrin  $\alpha_{IIb}\beta_3$ . *Blood* **2002**, *99*, 151–158.
- Mazzucato, M.; Pradella, P.; Cozzi, M. R.; De, M. L.; Ruggeri, Z. M. Sequential Cytoplasmic Calcium Signals in a 2-Stage Platelet Activation Process Induced by the Glycoprotein Ib $\alpha$  Mechanoreceptor. *Blood* **2002**, *100*, 2793–2800.
- Nesbitt, W. S.; Kulkarni, S.; Giuliano, S.; Goncalves, I.; Doppeide, S. M.; Yap, C. L.; Harper, I. S.; Salem, H. H.; Jackson, S. P. Distinct Glycoprotein Ib/V/IX and Integrin  $\alpha_{IIb}\beta_3$ -Dependent Calcium Signals Cooperatively Regulate Platelet Adhesion under Flow. *J. Biol. Chem.* **2002**, *277*, 2965–2972.
- Kubik, T.; Bogunia-Kubik, K.; Sugisaka, M. Nanotechnology on Duty in Medical Applications. *Curr. Pharm. Biotechnol.* **2005**, *6*, 17–33.
- Bhirde, A. A.; Patel, V.; Gavard, J.; Zhang, U.; Sousa, A. A.; Masedunskas, A.; Leapman, R. D.; Weigert, R.; Gutkind, J. S.; Rusling, J. F. Targeted Killing of Cancer Cells *in Vivo* and *in Vitro* with EGF-Directed Carbon Nanotube-Based Drug Delivery. *ACS Nano* **2009**, *3*, 307.
- Liao, H.; Nehl, C. L.; Hafner, J. H. Biomedical Applications of Plasmon Resonant Metal Nanoparticles. *Nanomedicine* **2006**, *1*, 201–208.
- Huang, X.; Jain, P.; El-Sayed, I. H.; El-Sayed, M. A. Gold Nanoparticles: Interesting Optical Properties and Recent Applications in Cancer Diagnostics and Therapy. *Nanomedicine* **2007**, *2*, 681–693.
- Silva, G. A. Introduction to Nanotechnology and Its Applications to Medicine. *Surg. Neurol.* **2004**, *61*, 216–220.

18. Brooking, J.; Davis, S. S.; Illum, L. Transport of Nanoparticles across the Rat Nasal Mucosa. *J. Drug Target.* **2001**, *9*, 267–279.
19. Shrivastava, S.; Bera, T.; Roy, A.; Singh, G.; Ramchandrarao, P.; Dash, D. Characterization of Enhanced Antibacterial Effect of Novel Silver Nanoparticles. *Nanotechnology* **2007**, *18*, 225103–225111.
20. Oberdorster, G.; Sharp, Z.; Atudorei, V.; Elder, A.; Gelein, R.; Kreyling, W.; Cox, C. Translocation of Inhaled Ultrafine Particles to the Brain. *Inhal. Toxicol.* **2004**, *16*, 437–445.
21. Fu, J.; Ji, J.; Fan, D.; Shen, J. Construction of Antibacterial Multilayer Films Containing Nanosilver via Layer-by-Layer Assembly of Heparin and Chitosan–Silver Ion Complex. *J. Biomed. Mater. Res. A* **2006**, *79*, 665–674.
22. Ji, J. H.; Jung, J. H.; Kim, S. S.; Yoon, J. U.; Park, J. D.; Choi, B. S.; Chung, Y. S.; Kwon, I. H.; Jeong, J.; Han, B. S.; Shin, J. H.; Sung, J. H.; Song, K. S.; Yu, I. J. Twenty-Eight-Day Inhalation Toxicity Study of Silver Nanoparticles in Sprague–Dawley Rats. *Inhal. Toxicol.* **2007**, *19*:10, 857–871.
23. Lansdown, A. B. Silver in Health Care: Antimicrobial Effects and Safety in Use. *Curr. Probl. Dermatol.* **2006**, *33*, 17–34.
24. Chen, X.; Schluesener, H. J. Nanosilver: A Nanoproduct in Medical Application. *Toxicol. Lett.* **2008**, *176*, 1–12.
25. White, J. M.; Powell, A. M.; Brady, K.; Russell-Jones, R. Severe Generalized Argyria Secondary to Ingestion of Colloidal Silver Protein. *Clin. Exp. Dermatol.* **2003**, *28*, 254–256.
26. Panyala, N. R.; Pena-mendez, E. M.; Havel, J. Silver or Silver Nanoparticles: A Hazardous Threat to the Environment and Human Health. *J. Appl. Biomed.* **2008**, *6*, 117–129.
27. Ansary, A. E.; Daihan, S. A. On the Toxicity of Therapeutically Used Nanoparticles: An Overview. *J. Toxicol.* 2009, doi: 10.1155/2009/754810.
28. Hussain, S. M.; Hess, K. L.; Gearhart, J. M.; Geiss, K. T.; Schlager, J. J. *In Vitro* toxicity of nanoparticles in BRL 3A rat liver cells. *Toxicol. Vitro* **2005**, *19*, 975–983.
29. Hussain, S. M.; Javorina, M. K.; Schrand, A. M.; Duhart, H. M.; Ali, S. F.; Schlager, J. J. The Interaction of Manganese Nanoparticles with PC-12 Cells Induces Dopamine Depletion. *Toxicol. Sci.* **2006**, *92*, 456–463.
30. Braydich-Stolle, L.; Hussain, S.; Schlager, J. J.; Hofmann, M. C. *In vitro* Cytotoxicity of Nanoparticles in Mammalian Germline Stem Cells. *Toxicol. Sci.* **2005**, *88*, 412–419.
31. Radomski, A.; Jurasz, P.; Escolano, D. A.; Drews, M.; Morandi, M.; Malinski Radomski, M. W. Nanoparticle-Induced Platelet Aggregation and Vascular Thrombosis. *Br. J. Pharmacol.* **2005**, *146*, 882–893.
32. Kim, Y. S.; Kim, J. S.; Cho, H. S.; Rha, D. S.; Kim, J. M.; Park, J. D.; Choi, B. S.; Lim, R.; Chang, H. K.; Chung, Y. H.; Kwon, I. H.; Jeong, J.; Han, B. S.; Yu, I. J. Twenty-Eight Day Oral Toxicity, Genotoxicity, and Gender-Related Tissue Distribution of Silver Nanoparticles in Sprague–Dawley Rats. *Inhal. Toxicol.* **2008**, *20*, 575–583.
33. Osdoit, S.; Rosa, J. P. Fibrin Clot Retraction by Human Platelets Correlates with  $\alpha_{IIb}\beta_3$  Integrin-Dependent Protein Tyrosine Dephosphorylation. *J. Biol. Chem.* **2001**, *276*, 6703–6710.
34. Litvinov, R. I.; Nagaswami, C.; Vilaire, G.; Shuman, H.; Bennett, J. S.; Weisel, J. W. Functional and Structural Correlations of Individual  $\alpha_{IIb}\beta_3$  Molecules. *Blood* **2004**, *104*, 3979–3985.
35. Salgado, E. G. A.; Haj, F.; Dubois, C.; Moran, B.; Friede, A. K.; Furie, B. C.; Furie, B.; Neel, B. G.; Shattil, S. J. PTP-1B is an Essential Positive Regulator of Platelet Integrin Signaling. *J. Cell. Biol.* **2005**, *170*, 837–845.
36. Fox, J. E. B.; Boyles, J. K.; Reynolds, C. C.; Phillips, D. R. Actin Filament Content and Organization in Unstimulated Platelets. *J. Cell. Biol.* **1984**, *98*, 1985–1991.
37. Hartwig, J. H. Mechanisms of Actin Rearrangements Mediating Platelet Activation. *J. Cell. Biol.* **1992**, *118*, 1421–1442.
38. Barkalow, K.; Witke, W.; Kwiatkowski, D. J.; Hartwig, J. H. Coordinated Regulation of Platelet Actin Filament Barbed Ends by Gelsolin and Capping Protein. *J. Cell. Biol.* **1996**, *134*, 389–399.
39. Dash, D.; Rao, G. R. K. Characterization of the Effects of Propranolol on the Physical State of Platelet Membrane. *Arch. Biochem. Biophys.* **1990**, *276*, 343–347.
40. Jiang, W.; Kim, B. Y. S.; Rutka, J. T.; Chan, W. C. W. Nanoparticle-Mediated Cellular Response Is Size-Dependent. *Nat. Nanotechnol.* **2008**, *3*, 145–150.
41. Chithrani, B. D.; Chan, W. C. W. Elucidating the Mechanism of Cellular Uptake and Removal of Protein-Coated Gold Nanoparticles of Different Sizes and Shapes. *Nano Lett.* **2007**, *7* (6), 1542–1550.
42. Medina, C.; Santos-Martinez, M. J.; Radomski, A.; Corrigan, O. I.; Radomski, M. W. Nanoparticles: Pharmacological and Toxicological Significance. *Br. J. Pharmacol.* **2007**, *150*, 552–558.
43. Gupta, R.; Chakrabarti, P.; Dikshit, M.; Dash, D. Late Signaling in the Activated Platelets Upregulates Tyrosine Phosphatase SHP1 and Impairs Platelet Adhesive Function: Regulation by Calcium and Src Kinase. *Biochim. Biophys. Acta* **2007**, *1773*, 131–140.
44. Podolnikova, N. P.; Yakubenko, V. P.; Volkov, G. L.; Plow, E. F.; Ugarova, T. P. Identification of a Novel Binding Site for Platelet Integrin  $\alpha_{IIb}\beta_3$  (GPIIb/IIIa) and  $\alpha_5\beta_1$  in the  $\gamma$ C-Domain of Fibrinogen. *J. Biol. Chem.* **2003**, *278*, 32251–32258.
45. Gryniewicz, G.; Poenie, M.; Tsien, R. Y. A New Generation of  $Ca^{2+}$  Indicators with Greatly Improved Fluorescence Properties. *J. Biol. Chem.* **1985**, *260*, 3440–3450.
46. Flaumenhaft, R.; Dilks, J. R.; Rozenvayn, R.; Monahan-Earley, R. A.; Feng, D.; Dvorak, A. M. The Actin Cytoskeleton Differentially Regulates Platelet  $\alpha$ -Granule and Dense-Granule Secretion. *Blood* **2005**, *105*, 3879–3887.
47. Dvorak, A. M. Monograph: Procedural Guide to Specimen Handling for the Ultrastructural Pathology Service Laboratory. *J. Electron Microsc. Technol.* **1987**, *6*, 255–301.